Simulation of 1D Topological Phases in Driven Quantum Dot Arrays

Beatriz Pérez-González,* Miguel Bello, Gloria Platero, and Álvaro Gómez-León
Instituto de Ciencia de Materiales de Madrid (ICMM-CSIC), E-28049 Madrid, Spain

(Received 25 March 2019; published 16 September 2019)

We propose a driving protocol which allows us to use quantum dot arrays as quantum simulators for 1D topological phases. We show that by driving the system out of equilibrium, one can imprint bond order in the lattice (producing structures such as dimers, trimers, etc.) and selectively modify the hopping amplitudes at will. Our driving protocol also allows for the simultaneous suppression of all the undesired hopping processes and the enhancement of the necessary ones, enforcing certain key symmetries which provide topological protection. In addition, we have discussed its implementation in a 12-QD array with two interacting electrons and found correlation effects in their dynamics, when configurations with different number of edge states are considered.

DOI: 10.1103/PhysRevLett.123.126401

Introduction.—Topological matter, and in particular topological insulators (TIs) [1–3], are materials of interest due to the presence of topologically protected surface states, robust to local perturbations. Consequently, a great effort is being made to simulate the behavior of TIs by tailoring other quantum systems, whose properties can be more easily controlled. Within this context, time-dependent modulations have proven to be useful tools to modify the topology [4–15]. Particularly, they have been used to simulate the so-called "Floquet topological insulators" (FTIs) [16–18] upon different systems [18–39].

Quantum dots (QDs) have revealed themselves as highly tunable quantum systems [40–43], in which both on-site energies [44] and couplings [45,46] can be independently addressed. This makes them an interesting platform for quantum simulation [47–49]. Recent experimental evidence on scalable quantum dot devices [50,51] demonstrates reproducible and controllable long QD arrays, which opens up new possibilities of simulating 1D TIs.

In this work we show that a quantum simulator for 1D topological phases can be obtained by periodically driving an array of QDs with long-range hopping. We propose a driving protocol which allows us to imprint bond order in the lattice [52], while also offers tunability for the long-range hoppings. This control can lead to configurations that would be unreachable otherwise, while preserving the fundamental symmetries which guarantee topological features. Thus, the driving protocol triggers nonequilibrium topological behavior in a trivial setup, opening the door to the simulation of different topological phases. We also study the exact time evolution for the case of two interacting electrons, and show that their dynamics can become highly correlated. This allows us to discriminate between different topological phases and also opens up new possibilities for quantum state transfer protocols. Our proposal can also be implemented in other setups as cold atoms or trapped ions [53–60].

Model.—We consider a Hamiltonian describing a periodically driven chain of QDs:

$$H(t) = \sum_{|i-j|\leq R} J_{ij} c_i^\dagger c_j + \sum_i A_i f(t) c_i^\dagger c_i \equiv H_{\text{array}} + H_{\text{driv}}(t), \tag{1}$$

where $c_i^\dagger$ (c_i) is the creation (destruction) operator for a spinless fermion at the ith site of the array. The first term represents the static Hamiltonian for a QD array of N sites, with J_{ij} being the real hopping amplitude connecting the ith and jth dots. Note that long-range hoppings are allowed to take place, up to range R. We will assume that hopping amplitudes in the undriven system decay monotonically as a function of the distance between sites, $J_{ij} = J(|i-j|)$. The second term in Eq. (1), $H_{\text{driv}}(t)$, corresponds to a time-periodic modulation of the on-site potentials A_i with $f(t) = f(T+t)$, and frequency $\omega = 2\pi/T$.

Regarding the simulation of 1D topological phases in QD arrays, the purpose of the time-periodic modulation is threefold. First, the driving must generate bond order, which is a crucial ingredient in toy models such as the SSH [61]. Second, certain neighbor hoppings can be simultaneously suppressed through the so-called coherent destruction of tunneling [62,63]. This difficult requirement turns out to be feasible when our driving protocol is included, and it is crucial to generate the necessary symmetries for the topological protection. Finally, other hoppings can be enhanced to be able to explore topological sectors with larger topological invariant.

All these objectives can be achieved through a spatially modulated square ac field [64–66]

$$f(t) = \begin{cases} -1 & \text{if } 0 \le t < T/2 \\ 1 & \text{if } T/2 \le t < T \end{cases}, \tag{2}$$

and, in particular, the simulation of an effective dimer lattice with long-range hopping can be realized by choosing the A_i in a stairlike fashion,

$$A_{2n} = n(\alpha+\beta), \qquad A_{2n-1} = n(\alpha+\beta) - \alpha, \tag{3}$$

with $n = 1, 2, 3, \ldots$, which translates into an alternating difference between two consecutive sites, namely, $A_{2n} - A_{2n-1} = \alpha$ and $A_{2n+1} - A_{2n} = \beta$. Given the time periodicity of the Hamiltonian $H(t) = H(t+T)$ [67,68], we can take advantage of Floquet theory to solve the time-dependent Schrödinger equation. The solutions take the form $|\psi_n(t)\rangle = e^{-i\epsilon_n t}|u_n(t)\rangle$, where the so-called Floquet modes $|u_n(t)\rangle = |u_n(t+T)\rangle$ have the same periodicity as the Hamiltonian, and ϵ_n are the so-called quasienergies, which play an analogous role to the energies in the static Hamiltonians. In the high-frequency regime ($\omega \gg J_0$), the dynamics is essentially dictated by the stroboscopic evolution of an effective time-independent Hamiltonian H_{eff}, which can be derived with a Magnus expansion. This leads to an effective Hamiltonian identical to H_{array}, but with renormalized hopping amplitudes [69]

$$J_{ij} \to \tilde{J}_{ij} = J_{ij} \frac{i\omega}{\pi(A_i - A_j)} [e^{-i\pi(A_i - A_j)/\omega} - 1]. \tag{4}$$

From Eq. (4) we can see that even-neighbor hoppings $J_{i,i\pm 2m}$ with $m = 1, 2, 3, \ldots$ ($\pm$ for hoppings to the right and left, respectively) renormalize through $A_i - A_{i\pm 2m} = \mp m(\alpha+\beta)$. This is important, because topological phases with chiral symmetry are spoiled by the presence of hoppings connecting sites within the same sublattice. The quenching of all $\tilde{J}_{i,i\pm 2m}$ can be achieved by choosing $\alpha + \beta = 2\omega q$, with $q = 0, 1, 2, \ldots$. Hence, chiral symmetry is recovered, regardless the maximum range of the hoppings included.

On the other hand, the renormalization of odd-neighbor hoppings leads to bond ordering, due to the alternating structure of the driving protocol. Together with the presence of chiral symmetry, this ensures the existence of distinct topological phases. We identify the renormalized $J_{2i,2i-r}$ as $\tilde{J}_{-r}{}'$ and $J_{2i+r,2i}$ as $\tilde{J}_r$ ($r \in [1, 3, 5, \ldots, R]$), obtaining [69]

$$\tilde{J}'_{-r} = \frac{iJ_{2i,2i-r}}{\pi[\frac{\alpha}{\omega} + (r-1)q]} [e^{-i\pi(\alpha/\omega + (r-1)q)} - 1],$$
$$\tilde{J}_r = \frac{iJ_{2i+r,2i}}{\pi[(r+1)q - \frac{\alpha}{\omega}]} [e^{-i\pi((r+1)q - (\alpha/\omega))} - 1]. \tag{5}$$

Notice that now long-range odd hoppings can be tuned, while keeping even hoppings suppressed. This can make long-range hoppings dominate over short-range ones, and then allows us to explore different topological phases by just tuning the driving amplitudes. The sign of r in the subscript is relevant since hopping amplitudes are now complex functions, and hence $\tilde{J}^{(\prime)}_{\pm r} = (\tilde{J}^{(\prime)}_{\mp r})^*$.

Interestingly, our protocol can be generalized to reproduce different kinds of bond ordering and to enforce other symmetries as well by choosing the driving on-site amplitudes accordingly. A trimer chain [71] is a particular example of a 1D system hosting nontrivial topological phases that can be realized in our setup. In this case, chiral symmetry is intrinsically absent, but the presence of another crystalline symmetry, space-inversion symmetry, can provide for topological protection [72]. A trimer chain can be realized in a QD driven monomer chain just by considering $A_{2n} - A_{2n-1} = A_{2n+1} - A_{2n} = \alpha$ and $A_{2n+2} - A_{2n+1} = \beta$.

Topological phase diagram for driven QD arrays.—In QD arrays, the bare hopping amplitudes typically decay exponentially with distance, with a decay length λ: $J_{ij} = Je^{-d_{ij}/\lambda}$, where d_{ij} is the distance between the ith and jth dots and J is of the order of tens of μeV, which are the typical energy scales in these setups. The distance between two consecutive QDs is set to $a = 1/2$ so that the unit cell in the effective dimerized chain is 1. By varying the value of α and λ in the driven system, topological phases with different topological invariant can be realized (Fig. 1). The topological invariant $\mathcal{W}$ is calculated as the winding number of the Bloch vector $\vec{d}(k) = (\text{Re}[d(k)], -\text{Im}[d(k)])$ around the origin [73], assuming a system with periodic boundary conditions, with $d(k)$ defined as

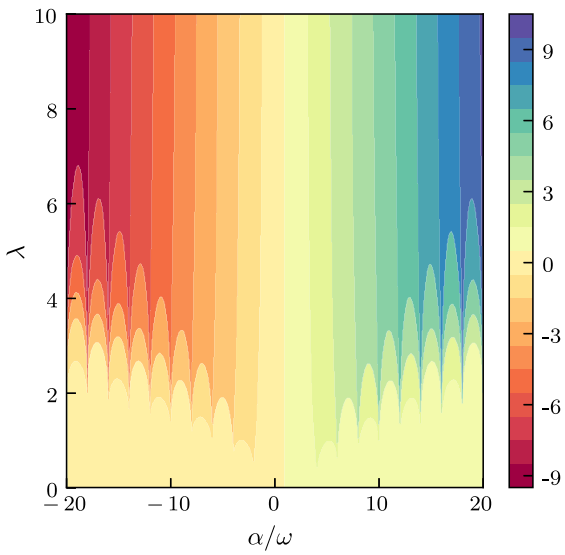

FIG. 1. Topological invariant $\mathcal{W}$ as a function of the driving amplitude α/ω and decay length of hopping amplitudes λ, for $q = 1$. The maximum range of the hoppings included is fixed by λ, such that the smallest bare hopping amplitude is a factor 10^{-8} smaller than the largest one.

$$d(k) = \sum_{r=1}^{R} \{\tilde{J}'_{-r} e^{ik[(r-1)/2]} + (\tilde{J}_r)^* e^{-ik[(r+1)/2]}\}. \quad (6)$$

For small values of λ, only $\mathcal{W} = 1$ and $\mathcal{W} = 0$ phases are allowed for all values of α/ω, since first-neighbor hoppings are dominant (this corresponds to the SSH model). Then, when λ is increased, other phases with larger $\mathcal{W}$ are possible, as a function of the ratio α/ω (we have also calculated the size of the gap in the Supplemental Material [69], as one is typically interested in gap sizes smaller than the temperature of the setup).

Typically, other driving protocols have been considered in the literature, such as sinusoidal driving fields $f(t) = \sin(\omega t + \phi)$ [8,10,11,27], or standing waves $f(t) = \cos(\omega t)\cos(kx_j + \phi)$ [74]. However, none of them would be suitable for engineering arbitrary chiral topological phases. In both previous cases, renormalization of the hopping amplitudes occurs through a zero-order Bessel function, whose roots are not periodically spaced. Hence, it would not be possible to suppress all even hoppings at once, and chiral symmetry would not be present.

The experimental evidence provided in Ref. [50] demonstrates a reproducible and controllable 12-quantum-dot device. Motivated by this experimental setup, we propose the implementation of our driving protocol in an array of 12 quantum dots. In Fig. 2 we show the quasienergies, as given by the effective Hamiltonian, of a driven 12-quantum-dot array, as a function of α/ω, with first- and third-neighbor hoppings (second-neighbor hoppings were initially present, but are effectively suppressed by the driving protocol), fixing $\lambda = 1.5$. The spectrum shows two topological phases with $\mathcal{W} = 1$ and $\mathcal{W} = 2$.

Dynamics of two interacting particles.—The number of edge states hosted by a finite system and their localization properties determine the motion of charges along the chain. Then, for an electron initially occupying the ending site, one would see oscillations between the two edges of the chain, with a frequency defined by the energy splitting $\omega_{\mathrm{osc}} \propto E_+ - E_-$, $E_\pm$ being the energy of each edge state in the pair. Hence, one can discriminate between topological phases with different numbers of edge states by studying the electron dynamics.

These ideas are illustrated in Fig. 3, where we consider two electrons with opposite spin loaded in a driven array of 12 QDs in such a way that the spin-up (spin-down) particle, which we will denote as $\uparrow$ ($\downarrow$), initially occupies the first (third) site. We have also included a local interaction term, being the total Hamiltonian,

$$H_{\uparrow\downarrow}(t) = \sum_{\sigma} \sum_{|i-j|\leq R} J_{ij} c^{\dagger}_{i,\sigma} c_{j,\sigma} + \sum_{i,\sigma} A_i f(t) n_{i,\sigma} + U \sum_i n_{i,\uparrow} n_{i,\downarrow}, \quad (7)$$

where $\sigma = \uparrow, \downarrow$. We do not include any spin-flip terms, since experimental evidence on silicon QDs confirms that the spin relaxation time within these QD structures is very long compared with the other energy scales of the system [75]. The A_i are chosen as indicated before, and α is fixed such that the system hosts either two or four edge states.

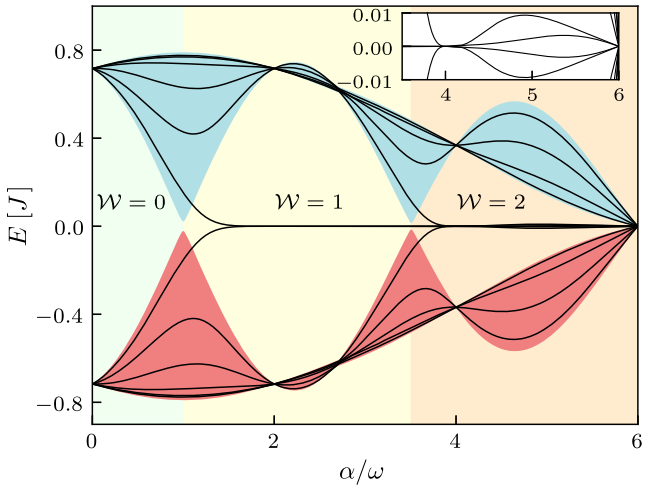

FIG. 2. Quasienergy levels of a driven 12-quantum dot array and band structure in the thermodynamical limit (red and blue filling for the valence and conduction band, respectively), as a function of α/ω, including first- and third-neighbor hoppings, in the high-frequency regime. Second-neighbor hoppings have been suppressed through the driving protocol. The parameters are $\lambda/\omega = 1.5$, $q = 1$. Inset: each pair of edge states in the $\mathcal{W} = 2$ phase has a different energy splitting, which can be also varied by tuning α/ω.

Then, the dynamics is exactly calculated from the time evolution operator $U(t,0) = e^{-i\int_0^t H_{\uparrow\downarrow} dt}$. Since $H_{\uparrow\downarrow}$ is time independent in each half period, the time-evolution operator $U(T,0)$ can be factorized into two independent time-evolution operators, $U(T,0) = U(T) = U_+(T/2)U_-(T/2)$, where the subscript $\pm$ corresponds to the sign of $f(t)$ in each of them. We choose for our simulations $\omega \gg J$ in order to accurately match the analytic expression in Eq. (5); however we have checked that values $\omega \gtrsim J$ still produce the expected behavior.

First, α is chosen such that the system hosts one pair of edge states ($\mathcal{W} = 1$ for the left half of Fig. 3), which have the largest weight at the ending sites of the chain. When interaction is turned off, particle $\uparrow$ oscillates between the ends of the chain, while particle $\downarrow$ spreads along the chain: at the third site, other states from the bulk have a non-negligible contribution and the edge states do not dominate the dynamics. When α is fixed so that the system has four edge states ($\mathcal{W} = 2$ for the right half of Fig. 3), one of the pairs is maximally localized at the first and last sites, while the other has the largest weight at the third and second-to-last sites. Hence, each particle is coupled to a different pair of edge states and it displays oscillations between different sites. The frequency of oscillation is also different, since each pair has a different energy splitting

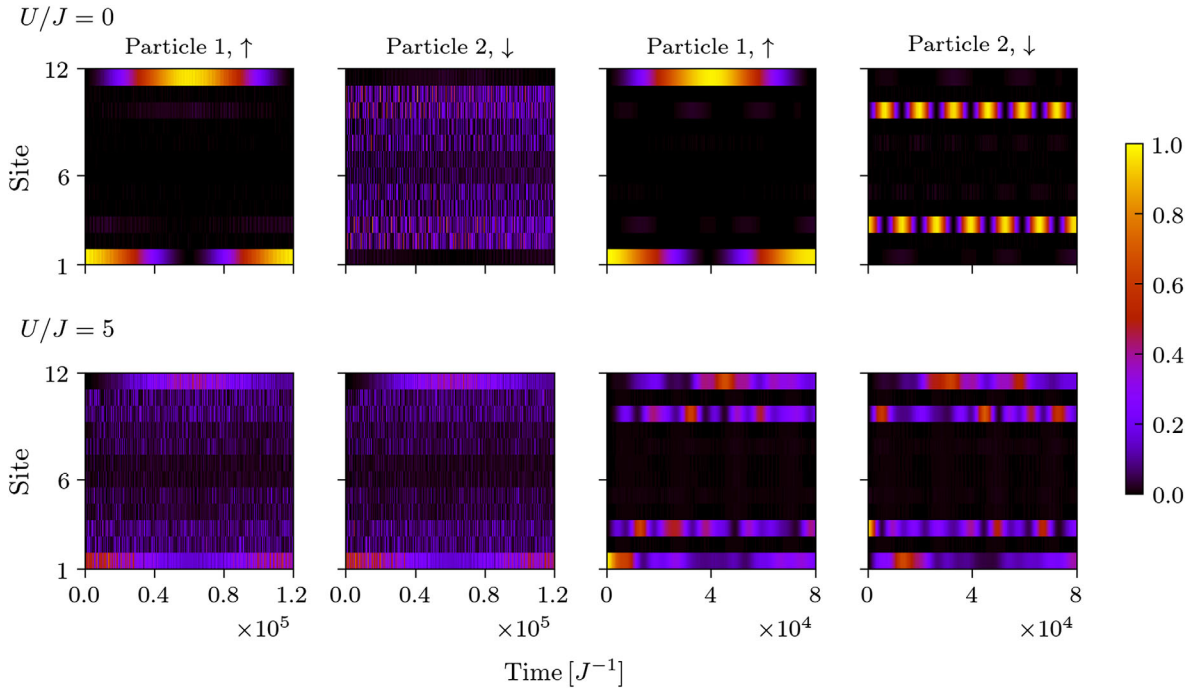

FIG. 3. Occupation of each site of a driven 12-QD array as a function of time when two electrons with opposite spin are loaded into the system, for different values of U. The array has first- to third-neighbor couplings, whose values initially decay exponentially with distance, choosing $\lambda = 1.5$. Considering the high-frequency regime with $\omega = 100$ and $q = 1$, the values for α have been chosen such that the desired hopping renormalization is realized. The four left plots correspond to $\alpha = 230$, resulting in a topological phase with $\mathcal{W} = 1$ (two edge states). The four right plots correspond to $\alpha = 410$, yielding a configuration with $\mathcal{W} = 2$ (four edge states).

(see inset in Fig. 2). The second pair has a bigger splitting and thus oscillations for particle ↓ happen faster.

Interestingly, for the case of nonvanishing local interaction one can see that the general effect is to correlate the dynamics of the two electrons. For the case of just one pair of edge states, the interaction correlates the edge mode with the bulk. They exchange spectral weight and oscillate coherently. However the case of two pairs of edge modes is more interesting, as the interaction correlates their dynamics, modifying the frequency of the oscillation while maintaining the edge modes isolated from the bulk. Notice that in both cases the frequency of oscillations changes, which is expected due to the nonlinear corrections produced by the interaction.

This difference in the exact dynamics for two particles confirms the method proposed in this work to engineer topological phases and provides a way to characterize them by detecting the time evolution of the charge occupation in the system.

Additionally, it is known that the edge states hosted by an SSH finite chain with nontrivial topology allow for long-range transfer of doublons directly from one end to the other without populating the intermediate region [4]. Here we show that the two-electron states can be directly transferred between outer dots by considering topological models with a larger winding number. Then, the presence of more pairs of edge states, which can be controlled by choosing a suitable value for α/ω, opens up the possibility of designing new quantum-state-transfer protocols.

Conclusions.—We have proposed a driving protocol to engineer topological phases in a QD array with exponentially decaying hoppings. This is achieved by spatially modulating the driving amplitudes to imprint bond ordering, and by selective enhancement or suppression of the different hopping processes. This generates the necessary symmetries for topological protection. We have simulated a dimerized chain with chiral symmetry by setting stairlike driving amplitudes and dynamically quenching even hoppings. Furthermore, our protocol allows us to enhance odd long-range hoppings versus short-range ones, thus opening the door to explore topological phases with different $\mathcal{W}$. The use of square pulses allows for a highly selective tunability of the different hoppings, where standard Floquet approaches using harmonic pulses would fail.

For the experimental implementation, scalable QD arrays of increasing size have been recently fabricated [50,51], making our proposal feasible with state of the art techniques.

To test our results we have simulated the exact dynamics for an initial product state, including local Coulomb interaction. We show that charge dynamics, which can be measured with quantum detectors in QD setups, discriminates between different topological phases. Additionally, we have found that the interplay of driving and interactions

produces a drag effect between the electrons, which forms correlated edge modes; this is not only of fundamental interest but also relevant for quantum simulation and information purposes.

Importantly, our protocol can also be implemented in other platforms, or even straightforwardly extended to 2D systems. The main requirement is the local control of the driving amplitude at each site. In optical lattices [53,54] this could be done with additional lasers [55], and the engineering of long-range hoppings is well suited in this case by selection of certain optical transitions [56]. In this setup, different topological features have been directly measured [57–60]. Trapped ions can also be used, as it is possible to locally address each ion, and their effective Hamiltonian can be reduced to that of single excitations with long-range hopping decaying as $\sim d^{-3}$ [74,76]. Finally, molecular patterning on surfaces by adsorbates could also be considered [77–81].

This work was supported by the Spanish Ministry of Economy and Competitiveness through Grant No. MAT2017-86717-P and we acknowledge support from CSIC Research Platform PTI-001. M. B. acknowledges the FPI Program No. BES-2015-071573, Á. G.-L. acknowledges the Juan de la Cierva program and B. P.-G. acknowledges the FPU Program No. FPU17/05297.

*bperez03@ucm.es

[1] C. L. Kane and E. J. Mele, Phys. Rev. Lett. **95**, 146802 (2005).
[2] M. Z. Hasan and C. L. Kane, Rev. Mod. Phys. **82**, 3045 (2010).
[3] X.-L. Qi and S.-C. Zhang, Rev. Mod. Phys. **83**, 1057 (2011).
[4] M. Bello, C. E. Creffield, and G. Platero, Sci. Rep. **6**, 22562 (2016).
[5] M. Bello, C. E. Creffield, and G. Platero, Phys. Rev. B **95**, 094303 (2017).
[6] M. Benito, A. Gómez-León, V. M. Bastidas, T. Brandes, and G. Platero, Phys. Rev. B **90**, 205127 (2014).
[7] Z.-Z. Li, C.-H. Lam, and J. Q. You, Phys. Rev. B **96**, 155438 (2017).
[8] M. Niklas, M. Benito, K. S, and G. Platero, Nanotechnology **27**, 454002 (2016).
[9] C. E. Creffield and G. Platero, Phys. Rev. B **69**, 165312 (2004).
[10] C. E. Creffield, Phys. Rev. Lett. **99**, 110501 (2007).
[11] D. Zueco, F. Galve, S. Kohler, and P. Hänggi, Phys. Rev. A **80**, 042303 (2009).
[12] J. Klinovaja, P. Stano, and D. Loss, Phys. Rev. Lett. **116**, 176401 (2016).
[13] L. Jiang, T. Kitagawa, J. Alicea, A. R. Akhmerov, D. Pekker, G. Refael, J. I. Cirac, E. Demler, M. D. Lukin, and P. Zoller, Phys. Rev. Lett. **106**, 220402 (2011).
[14] R. Aguado and G. Platero, Phys. Rev. B **55**, 12860 (1997).
[15] M. Thakurathi, A. A. Patel, D. Sen, and A. Dutta, Phys. Rev. B **88**, 155133 (2013).
[16] J. Cayssol, B. Dóra, F. Simon, and R. Moessner, Phys. Status Solidi **7**, 101 (2013).
[17] N. H. Lindner, G. Refael, and V. Galitski, Nat. Phys. **7**, 490 (2011).
[18] T. Oka and H. Aoki, Phys. Rev. B **79**, 081406(R) (2009).
[19] P. M. Perez-Piskunow, G. Usaj, C. A. Balseiro, and L. E. F. F. T. Torres, Phys. Rev. B **89**, 121401(R) (2014).
[20] G. Usaj, P. M. Perez-Piskunow, L. E. F. Foa Torres, and C. A. Balseiro, Phys. Rev. B **90**, 115423 (2014).
[21] E. Suárez Morell and L. E. F. Foa Torres, Phys. Rev. B **86**, 125449 (2012).
[22] Z. Gu, H. A. Fertig, D. P. Arovas, and A. Auerbach, Phys. Rev. Lett. **107**, 216601 (2011).
[23] P. Delplace, A. Gómez-León, and G. Platero, Phys. Rev. B **88**, 245422 (2013).
[24] M. Busl, G. Platero, and A.-P. Jauho, Phys. Rev. B **85**, 155449 (2012).
[25] P. M. Perez-Piskunow, L. E. F. Foa Torres, and G. Usaj, Phys. Rev. A **91**, 043625 (2015).
[26] A. Gómez-León, P. Delplace, and G. Platero, Phys. Rev. B **89**, 205408 (2014).
[27] A. Gómez-León and G. Platero, Phys. Rev. Lett. **110**, 200403 (2013).
[28] J.-i. Inoue and A. Tanaka, Phys. Rev. Lett. **105**, 017401 (2010).
[29] N. H. Lindner, D. L. Bergman, G. Refael, and V. Galitski, Phys. Rev. B **87**, 235131 (2013).
[30] V. Dal Lago, M. Atala, and L. E. F. Foa Torres, Phys. Rev. A **92**, 023624 (2015).
[31] Y. T. Katan and D. Podolsky, Phys. Rev. Lett. **110**, 016802 (2013).
[32] M. D. Reichl and E. J. Mueller, Phys. Rev. A **89**, 063628 (2014).
[33] I.-D. Potirniche, A. C. Potter, M. Schleier-Smith, A. Vishwanath, and N. Y. Yao, Phys. Rev. Lett. **119**, 123601 (2017).
[34] W. Zheng and H. Zhai, Phys. Rev. A **89**, 061603(R) (2014).
[35] M. Rechtsman, J. Zeuner, Y. Plotnik, Y. Lumer, D. Podolsky, F. Dreisow, S. Nolte, M. Segev, and A. Szameit, Nature (London) **496**, 196 (2013).
[36] R. Fleury, A. Khanikaev, and A. Alù, Nat. Commun. **7**, 11744 (2016).
[37] Y. Peng, C. Qin, D. Zhao, Y. Shen, X. Xu, M. Bao, H. Jia, and X. Zhu, Nat. Commun. **7**, 13368 (2016).
[38] V. Khemani, A. Lazarides, R. Moessner, and S. L. Sondhi, Phys. Rev. Lett. **116**, 250401 (2016).
[39] M. Bukov, L. D'Alessio, and A. Polkovnikov, Adv. Phys. **64**, 139 (2015).
[40] J. R. Petta, A. C. Johnson, J. M. Taylor, E. A. Laird, A. Yacoby, M. D. Lukin, C. M. Marcus, M. P. Hanson, and A. C. Gossard, Science **309**, 2180 (2005).
[41] K. D. Petersson, J. R. Petta, H. Lu, and A. C. Gossard, Phys. Rev. Lett. **105**, 246804 (2010).
[42] S. d'Hollosy, M. Jung, A. Baumgartner, V. A. Guzenko, M. H. Madsen, J. Nygård, and C. Schönenberger, Nano Lett. **15**, 4585 (2015).
[43] T. Tanttu, A. Rossi, K. Y. Tan, A. Mäkinen, K. W. Chan, A. S. Dzurak, and M. Möttönen, Sci. Rep. **6**, 36381 (2016).

[44] T. H. Oosterkamp, T. Fujisawa, W. G. van der Wiel, K. Ishibashi, R. V. Hijman, S. Tarucha, and L. P. Kouwenhoven, Nature (London) **395**, 873 (1998).
[45] F. Martins, F. K. Malinowski, P. D. Nissen, E. Barnes, S. Fallahi, G. C. Gardner, M. J. Manfra, C. M. Marcus, and F. Kuemmeth, Phys. Rev. Lett. **116**, 116801 (2016).
[46] M. D. Reed, B. M. Maune, R. W. Andrews, M. G. Borselli, K. Eng, M. P. Jura, A. A. Kiselev, T. D. Ladd, S. T. Merkel, I. Milosavljevic, E. J. Pritchett, M. T. Rakher, R. S. Ross, A. E. Schmitz, A. Smith, J. A. Wright, M. F. Gyure, and A. T. Hunter, Phys. Rev. Lett. **116**, 110402 (2016).
[47] T. Hensgens, T. Fujita, L. Janssen, X. Li, C. J. Van Diepen, C. Reichl, W. Wegscheider, S. Das Sarma, and L. M. K. Vandersypen, Nature (London) **548**, 70 (2017).
[48] A. Y. Smirnov, S. Savel'ev, L. G. Mourokh, and F. Nori, Europhys. Lett. **80**, 67008 (2007).
[49] J. Gray, A. Bayat, R. K. Puddy, C. G. Smith, and S. Bose, Phys. Rev. B **94**, 195136 (2016).
[50] D. M. Zajac, T. M. Hazard, X. Mi, E. Nielsen, and J. R. Petta, Phys. Rev. Applied **6**, 054013 (2016).
[51] C. Volk, A. M. J. Zwerver, U. Mukhopadhyay, P. T. Eendebak, C. J. van Diepen, J. P. Dehollain, T. Hensgens, T. Fujita, C. Reichl, W. Wegscheider, and L. M. K. Vandersypen, npj Quantum Inf. **5**, 29 (2019).
[52] H. Guo, Phys. Lett. A **378**, 1316 (2014).
[53] G. Gauthier, I. Lenton, N. M. Parry, M. Baker, M. J. Davis, H. Rubinsztein-Dunlop, and T. W. Neely, Optica **3**, 1136 (2016).
[54] D. Stuart and A. Kuhn, New J. Phys. **20**, 023013 (2018).
[55] C. Weitenberg, M. Endres, J. F. Sherson, M. Cheneau, P. Schauß, T. Fukuhara, I. Bloch, and S. Kuhr, Nature (London) **471**, 319 (2011).
[56] F. Meinert, M. J. Mark, E. Kirilov, K. Lauber, P. Weinmann, M. Gröbner, A. J. Daley, and H.-C. Nägerl, Science **344**, 1259 (2014).
[57] M. Atala, M. Aidelsburger, J. T. Barreiro, J. Abanin, T. Kitagawa, E. Demler, and I. Bloch, Nat. Phys. **9**, 795 (2013).
[58] D. Xie, W. Gou, T. Xiao, B. Gadway, and B. Yan, npj Quantum Inf. **5**, 55 (2019).
[59] E. J. Meier, F. A. An, and B. Gadway, Nat. Commun. **7**, 13986 (2016).
[60] X. Li, E. Zhao, and W. Vincent Liu, Nat. Commun. **4**, 1523 (2013).
[61] W. P. Su, J. R. Schrieffer, and A. J. Heeger, Phys. Rev. Lett. **42**, 1698 (1979).
[62] B. Pérez-González, M. Bello, A. Gómez-León, and G. Platero, Phys. Rev. B **99**, 035146 (2019).
[63] F. Grossmann, T. Dittrich, P. Jung, and P. Hänggi, Phys. Rev. Lett. **67**, 516 (1991).
[64] C. E. Creffield, Phys. Rev. B **67**, 165301 (2003).
[65] M. J. Zhu, X.-G. Zhao, and Q. Niu, J. Phys. Condens. Matter **11**, 4527 (1999).
[66] N. Goldman and J. Dalibard, Phys. Rev. X **4**, 031027 (2014).
[67] A. Eckardt and E. Anisimovas, New J. Phys. **17**, 093039 (2015).
[68] N. Goldman and J. Dalibard, Phys. Rev. X **4**, 031027 (2014).
[69] See Supplemental Material at http://link.aps.org/supplemental/10.1103/PhysRevLett.123.126401 for a detailed calculation of the high-frequency effective Hamiltonian, the renormalized hopping amplitudes, and the band gap as a function of the system parameters, which includes Ref. [70].
[70] T. Mikami, S. Kitamura, K. Yasuda, N. Tsuji, T. Oka, and H. Aoki, Phys. Rev. B **93**, 144307 (2016).
[71] V. M. Martinez Alvarez and M. D. Coutinho-Filho, Phys. Rev. A **99**, 013833 (2019).
[72] L. Fu and C. L. Kane, Phys. Rev. B **76**, 045302 (2007).
[73] P. Delplace, D. Ullmo, and G. Montambaux, Phys. Rev. B **84**, 195452 (2011).
[74] P. Nevado, S. Fernández-Lorenzo, and D. Porras, Phys. Rev. Lett. **119**, 210401 (2017).
[75] T. Fujisawa, D. G. Austing, Y. Tokura, Y. Hirayama, and S. Tarucha, Phys. Rev. Lett. **88**, 236802 (2002).
[76] P. Nevado and D. Porras, Phys. Rev. A **93**, 013625 (2016).
[77] S. N. Kempkes, M. R. Slot, S. E. Freeney, S. J. M. Zevenhuizen, D. Vanmaekelbergh, I. Swart, and C. M. Smith, Nat. Phys. **15**, 127 (2019).
[78] S. N. Kempkes, M. R. Slot, J. J. van den Broeke, P. Capiod, W. A. Benalcazar, D. Vanmaekelbergh, D. Bercioux, I. Swart, and C. Morais Smith,arXiv:1905.06053.
[79] M. R. Slot, T. S. Gardenier, P. H. Jacobse, G. C. P. van Miert, S. N. Kempkes, S. J. M. Zevenhuizen, C. M. Smith, D. Vanmaekelbergh, and I. Swart, Nat. Phys. **13**, 672 (2017).
[80] R. Drost, T. Ojanen, A. Harju, and P. Liljeroth, Nat. Phys. **13**, 668 (2017).
[81] M. Nurul Huda, S. Kezilebieke, T. Ojanen, R. Drost, and P. Liljeroth, arXiv:1806.08614.